Available online at www.sciencedirect.com
SCIENCE DIRECT
Journal of Nuclear Materials 351 (2006) 216–222
journal of nuclear materials
www.elsevier.com/locate/jnucmat

The effects of irradiation, annealing and reirradiation on RPV steels

M.K. Miller *, R.K. Nanstad, M.A. Sokolov, K.F. Russell

Microscopy, Microanalysis, Microstructure Group, Metals and Ceramics Division, Oak Ridge National Laboratory, P.O. Box 2008, Building 4500S, MS 6136, Oak Ridge, TN 37831-6136, USA

Abstract

An atom probe tomography microstructural characterization has been performed on an A533B pressure vessel steel (JRQ) after irradiation to a fluence of 5×10^{23} n m^{-2} ($E > 1$ MeV) and a subsequent annealing treatment of 168 h at 460 °C and also through two cycles of neutron irradiation (0.85×10^{23} n m^{-2} ($E > 1$ MeV)) and annealing (168 h at 460 °C). The alloy that was neutron irradiated to a fluence of 5×10^{23} n m^{-2} exhibited a high number density of Cu-enriched precipitates and a shift in the ductile-to-brittle transformation temperature of $\Delta T_{41J} = 96$ °C. Annealing for 168 h at 460 °C coarsened these Cu-enriched precipitates and recovered the embrittlement. The material that was re-irradiated to a total fluence 1.7×10^{23} n m^{-2} also exhibited a high number density of Cu-enriched precipitates and a ΔT_{41J} shift of 56 °C. Annealing the re-irradiated material for 168 h at 460 °C coarsened these precipitates and recovered the embrittlement.
Published by Elsevier B.V.

PACS: 61.82.Bg; 62.20.Mk; 81.40.−z

1. Introduction

Atom probe field ion microscopy and atom probe tomography have firmly established that a high number density of ultrafine copper-, manganese-, nickel- and silicon-enriched precipitates are produced in copper-containing pressure vessel steels during neutron irradiation [1,2]. These precipitates are a primary cause of the degradation in the mechanical properties of these materials during service in a nuclear reactor. Several studies have demonstrated that the mechanical properties of these steels may be recovered by annealing the pressure vessel at a temperature of ∼340 to ∼450 °C for a few days [2–12]. This annealing procedure permits the lifetime of the reactor to be extended.

An atom probe field ion microscopy (APFIM) study has been performed on a forging and weld materials from the B&W Owners Group containing 0.017 and 0.24 wt% Cu, respectively, after neutron irradiation to fluences of up to 3.5×10^{23} m^{-2} ($E > 1$ MeV) and thermal annealing for 168 h at 454 °C or 29 h at 610 °C [13]. This study revealed the formation of Cu-, Si-, Ni-, Mn-enriched clusters

* Corresponding author. Tel.: +1 865 574 4719; fax: +1 865 241 3650.
E-mail address: millermk@ornl.gov (M.K. Miller).

0022-3115/$ - see front matter Published by Elsevier B.V.
doi:10.1016/j.jnucmat.2006.02.010

during the irradiation and a decrease in the matrix copper level followed by dissolution and growth of these precipitates during the thermal anneal with a further decrease in the matrix copper level. Similar results were also obtained in an APFIM study of a weld from the Midland reactor that was irradiated to a fluence of 1.1×10^{23} m^{-2} ($E > 1$ MeV) and thermally annealed for 168 h at 454 °C [14].

An atom probe tomography (APT) study of a submerged arc weld (Weld 73 W) containing 0.16 wt% Cu in the matrix after the stress anneal that was irradiated to a fluence of 1.8×10^{23} m^{-2} ($E > 1$ MeV), thermally annealed for 168 h at 454 °C and reirradiated to an additional fluence of 0.8×10^{23} m^{-2} ($E > 1$ MeV) revealed the formation of Cu-, Si-, Ni-, Mn-enriched clusters during the initial irradiation, dissolution and growth of these precipitates during the thermal anneal, and the formation of some additional subnanometer diameter clusters after the reirradiation [15]. Another APT study of a 15Kh2MFA steel used in a VVER440 reactor containing 0.14 wt% Cu that was irradiated to a fluence of 9.7×10^{23} m^{-2} ($E > 0.5$ MeV), thermally annealed for 150 h at 475 °C and reirradiated to an additional fluence of 9.7×10^{23} m^{-2} ($E >$ 0.5 MeV) also revealed the formation of Cu-, Si-, Ni-, Mn- and P-enriched clusters during the initial irradiation, dissolution and growth of these precipitates during the thermal anneal, but no additional Cu-, Si-, Ni-, Mn- and P-enriched clusters were detected after the reirradiation [16]. Phosphorus segregation to dislocations was also observed in these studies.

In this atom probe tomography study, the number density, size, and composition of these ultrafine precipitates have been studied in a reference A533B steel (JRQ) after neutron irradiation to a relatively high fluence and an annealing treatment and also through two irradiation and annealing cycles.

2. Experimental

The composition of the JRQ steel used in this atom probe tomography study was Fe–0.14 wt % Cu, 0.18% C, 1.42% Mn, 0.84% Ni, 0.24% Si, 0.51% Mo, 0.12% Cr, and 0.017% P (Fe–0.12 at.% Cu, 0.83% C, 1.43% Mn, 0.79% Ni, 0.47% Si, 0.30% Mo, 0.13% Cr, and 0.03% P). The alloy was characterized after neutron irradiation to a fluence of 5×10^{23} n m^{-2} ($E > 1$ MeV) (I) in the 10 MW (thermal) SAPHIR reactor and after subsequent annealing for 168 h at 460 °C (IA). The alloy was also characterized after neutron irradiation to a fluence of 0.85×10^{23} n m^{-2} ($E > 1$ MeV), annealing for 168 h at 460 °C and reirradiation to a fluence of 0.85×10^{23} n m^{-2} ($E > 1$ MeV) (IAR). The annealing treatment was performed when 50% of the total target fluence of 1.7×10^{23} n m^{-2} ($E > 1$ MeV) was reached. This IAR material was also given a subsequent annealing treatment of 168 h at 460 °C (IARA). All irradiations were performed at a temperature of 288 °C.

These alloys were characterized with the Oak Ridge National Laboratory local electrode atom probe [17]. A specimen temperature of 50 K, a pulse repetition rate of 200 kHz and a pulse fraction of 20% were used for the analyses. This high pulse repetition rate significantly reduces the possibility of preferential evaporation of the low evaporation field solutes such as copper [18,19]. Compared to previous types of atom probes, this new instrument has a significantly larger field of view and hence larger volumes of analysis and faster rate of data acquisition.

Previous atom probe studies of these materials have revealed that the primary microstructural feature that changes during the irradiation and annealing cycles is the copper-enriched precipitates [1,2,20–27]. These precipitates are typically less than 5 nm in diameter. Therefore, the number of atoms associated with these features is extremely small and the proportion of atoms in the surface of the feature is large. Consequently, the estimation of their size, composition and number density is dependent to the precise definition of the extent of the feature. The presence of solute-enriched precipitates was determined with the maximum separation method [17,21]. This method is based on the premise that the distance between solute atoms in a solute-enriched precipitate is significantly smaller than that in the surrounding matrix. Therefore, the atoms that belong to a solute-enriched precipitate may be distinguished from those in the matrix based on a maximum separation distance, d_{max}. Computer simulations of random solid solutions containing 0.12% solute with a body centered cubic α-Fe crystal ($a_0 = 0.288$ nm) and a detection efficiency of 60% were used to define the value of $d_{max} = 0.6$ nm and the minimum number of solute atoms associated with each cluster, $n_{min} = 5$, to exclude fluctuations consistent with the random solid solution. The size of the solute-enriched features was estimated in terms of the radius of gyration, which was determined from positions of the solute atoms in each cluster. A correction was applied to account for the measured variation in the local magnification between the cluster and the matrix. The composition of each cluster was estimated with the envelope method with a grid spacing of 0.11 nm [17]. The number densities were estimated from the number of particles in the volume of analysis, where the volume was estimated from the number of atoms in the volume, the detection efficiency of the mass spectrometer and the atomic density of body centered cubic iron. These definitions should be taken into account when comparing these results with the results from other techniques.

3. Results and discussion

3.1. Mechanical properties

The Charpy impact test results of these materials exhibited typical irradiation-induced behaviour with fluence [28]. The T_{41J} temperatures of the unirradiated and neutron irradiated (I) conditions were estimated to be −28 °C and 68 °C, respectively. Therefore, the shift in the ductile-to-brittle transition temperature due to neutron irradiation to a fluence of 5×10^{23} n m^{-2} was 96 °C. The T_{41J} temperature of the neutron irradiated and annealed (IA) material was estimated from Reg. Guide 1.162 to be −22 °C. Therefore, the shift in the ductile-to-brittle transition temperature compared to the unirradiated alloy was ~6 °C. This result indicates that the mechanical properties were almost fully recovered after the thermal annealing treatment of 168 h at 460 °C. The fracture toughnesses of the irradiated (I) and irradiated and annealed (IA) materials are shown in Fig. 1. These curves also indicate full recovery of T_0 after the annealing treatment of 168 h at 460 °C.

The results of the Charpy impact tests of the unirradiated, IAR and IARA conditions are shown in Fig. 2. The T_{41J} temperatures of the IAR and IARA conditions were estimated to be 28 °C and −18 °C, respectively. The shift in the ductile-to-brittle transition temperature after reirradiation to a fluence of 0.85×10^{23} n m^{-2} and a total fluence of 1.7×10^{23} n m^{-2} was 56 °C indicating significant reembrittlement after the intermediate annealing treatment. The shift in the ductile-to-brittle transition temperature of the IARA condition compared to the unirradiated alloy was ~10 °C indicating that the mechanical properties were almost fully recovered after the second thermal annealing treatment

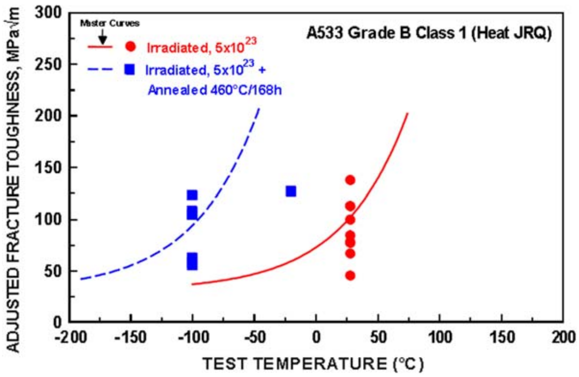

Fig. 1. Fracture toughness of the irradiated (I 5×10^{23} n m^{-2} ($E > 1$ MeV)) and irradiated and annealed (IA 5×10^{23} n m^{-2} ($E > 1$ MeV) and 168 h at 460 °C) materials.

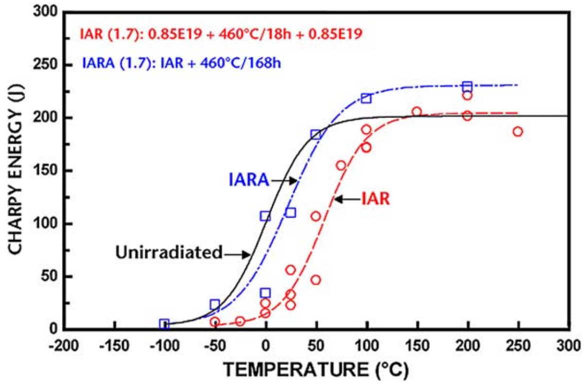

Fig. 2. Energy absorbed in fracture of the irradiated (0.85×10^{23} n m^{-2} ($E > 1$ MeV)), annealed (168 h at 460 °C) and reirradiated (0.85×10^{23} n m^{-2} ($E > 1$ MeV)) (IAR) and reirradiated and annealed (168 h at 460 °C) (IARA) materials.

of 168 h at 460 °C. The upper shelf energy was found to increase after the IARA treatment. Additional details of the mechanical properties are presented elsewhere [29–31].

3.2. Microstructure

No copper-enriched precipitates were observed in the unirradiated control material. The matrix copper level of the unirradiated control material was estimated to be 0.12 ± 0.01 at.% Cu. This value was the same as the alloy composition indicating that no significant amount of copper was consumed in coarse precipitates during the prior thermal processing of the alloy.

Atom probe tomography revealed that neutron irradiation (I) produced a high number density of

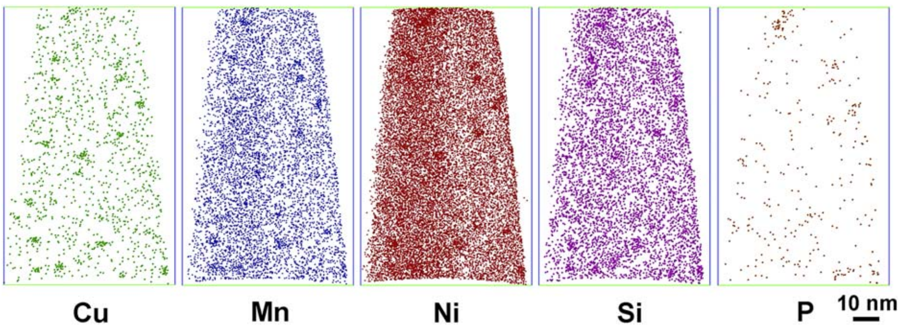

Fig. 3. Atom maps of the neutron irradiated material (I 5×10^{23} n m^{-2} ($E > 1$ MeV)) material. A high number density of Cu-, Mn-, Ni- and Si-enriched precipitates is evident.

ultrafine copper-, manganese-, nickel- and silicon-enriched precipitates, as shown in Fig. 3. The number density was estimated to be $\sim 3 \times 10^{23}$ m^{-3}. The average radius of gyration of the precipitates was estimated to be 1.1 ± 0.1 nm. The average composition of the core of these precipitates estimated by the maximum separation envelope method was Fe–87 ± 9% Cu with enriched levels of nickel, manganese, silicon and phosphorus. It is evident from the atom maps that the extent of the nickel, manganese and silicon was larger than that of copper. The matrix copper content of the neutron irradiated materials was reduced to 0.07 ± 0.01 at.% Cu from the unirradiated level of 0.12 ± 0.01 at.% Cu as a result of these copper-enriched precipitates. The high number density of these precipitates correlate

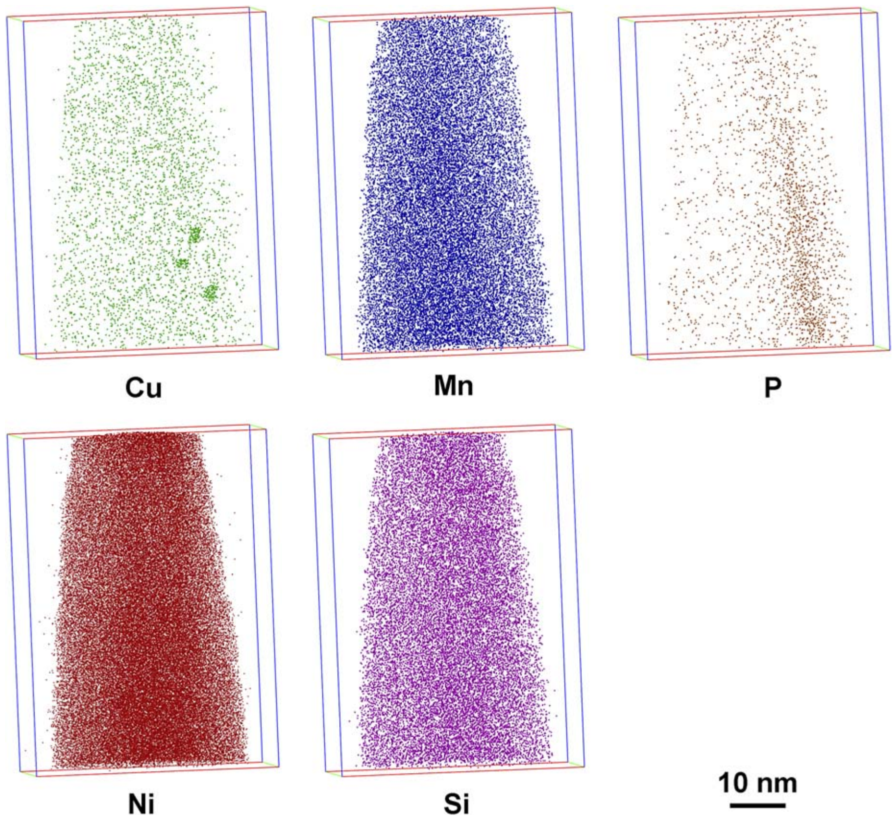

Fig. 4. Atom maps of the neutron irradiated 5×10^{23} n m^{-2} ($E > 1$ MeV) and annealed and 168 h at 460 °C (IA) material. A low number density of Cu-enriched precipitates is evident.

with the embrittlement of the steel and 96 °C shift in the ductile-to-brittle transition temperature.

After annealing at 460 °C (IA), the number density of these intragranular precipitates significantly decreased. Some copper-enriched precipitates were observed on a grain boundary, as shown in Fig. 4. The number density of these precipitates was $\sim 2 \times 10^{22}$ m^{-3}. The average radius of gyration of these precipitates was 1.5 ± 0.1 nm. A slight decrease in the matrix copper content to 0.06 ± 0.01 at.% Cu was also observed after the thermal annealing treatment. These results indicate that the precipitates did not redissolve into the matrix but coarsened. This coarsening process in conjunction with the irradiation removed a significant amount (50%) of copper from the matrix of the alloy so that only 0.06% Cu is available for the formation of additional precipitates during subsequent reirradiations. The number density of precipitates was sufficiently low that their influence on the mechanical properties was small. This result is in agreement with the previous atom probe studies [15].

After the irradiation, annealing and reirradiation (IAR) treatment, a high number density of significantly smaller copper-enriched precipitates was again observed, as shown in Fig. 5. The presence of these small precipitates correlates with the reembrittlement of the steel and the 56 °C shift in the ductile-to-brittle transformation temperature. The number density of these precipitates was estimated to be 1.3×10^{23} m^{-3}. The radius of gyration of these precipitates was estimated to be 0.9 ± 0.4 nm. The average number of atoms in these precipitates was 16 ± 9. The average composition of the core of the precipitates estimated by the maximum separation envelope method was Fe–93 ± 7% Cu. The matrix copper content was 0.09 ± 0.01 at.% Cu. This matrix content is slightly higher than that measured after the irradiated (I) condition due to the lower total fluence (5×10^{23} n m^{-2} compared to a total of 1.7×10^{23} n m^{-2} ($E > 1$ MeV)). Consequently, the time available for diffusion of copper atoms from the supersaturated matrix to the precipitates was shorter and resulted in a slightly higher matrix level. It is also possible that some sample to sample variation may account for some of this difference. Therefore, the difference (at least 0.03 at.% Cu) is available for the formation of additional precipitates and embrittlement during further neutron irradiation. If the first irradiation and annealing cycle does not remove the excess copper from the matrix, additional Cu-enriched precipitates form, which reembrittles the steel. The precise solubility level of copper in the ferrite matrix under neutron irradiation conditions where there is an enhanced vacancy concentration and enhanced diffusion has not been firmly established. However, several atom probe studies indicate that this level is less than $\sim$0.05% Cu. Therefore, the matrix copper content of the alloy, the stress relief treatment and the parameters (fluence, flux, temperature and time) of the first irradiation and the annealing treatment control copper content of the matrix and together with the parameters (fluence, flux, temperature and time) of the reirradiation control the level of reembrittlement.

A significantly lower number density of ultrafine copper-enriched precipitates was observed after the second annealing treatment (IARA), as shown in Fig. 6. However, some larger copper-rich precipitates were observed after this treatment. The number density of these precipitates was estimated to be $\approx 1 \times 10^{22}$ m^{-3}. The radius of gyration of the precipitate shown in Fig. 6 was 1.6 nm. These results indicate that the ultrafine precipitates did not redissolve into the matrix but coarsened.

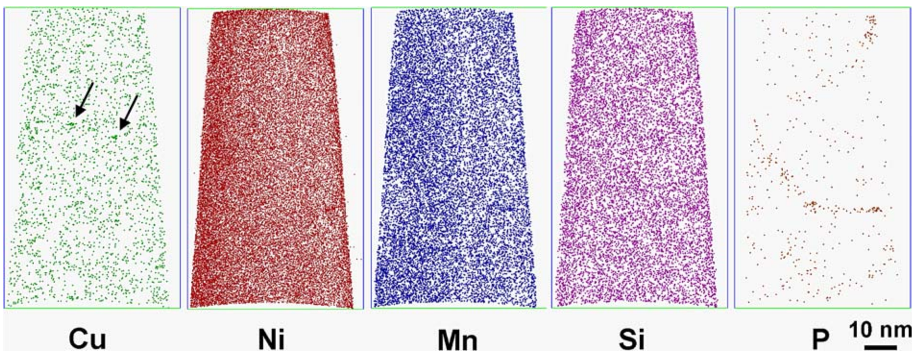

Fig. 5. Atom map of the IAR condition showing a distribution of ultrafine Cu-enriched precipitates.

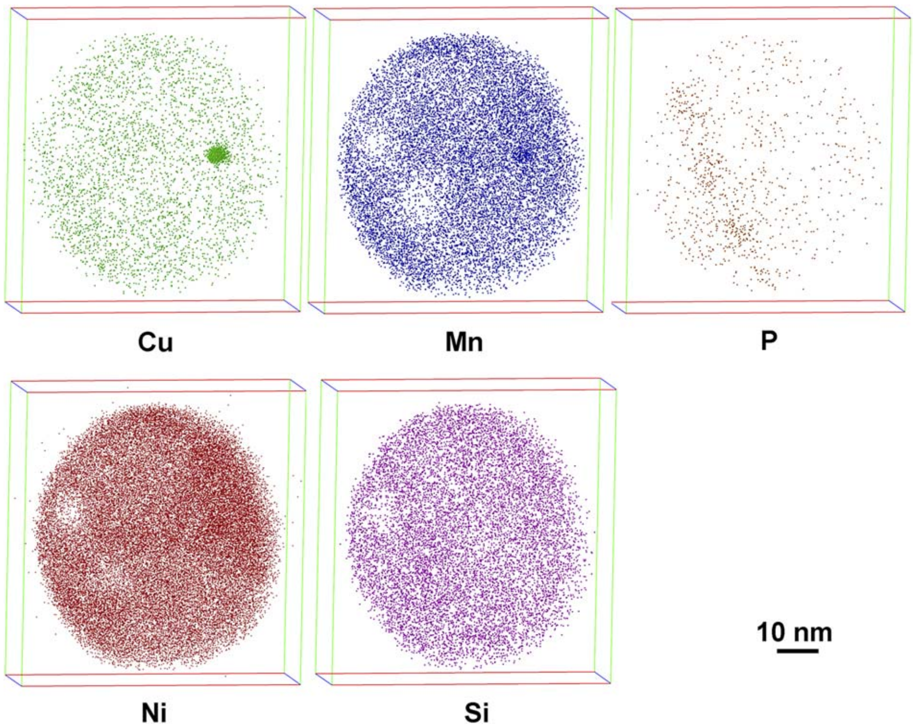

Fig. 6. Atom maps of the IARA condition showing a significant reduction in the number density of Cu-, Mn-, Ni- and Si-enriched precipitates.

Phosphorus segregation was also observed at dislocations in these materials.

4. Conclusions

This atom probe tomography microstructural characterization of an A533B pressure vessel steel (JRQ) revealed a high number density of Cu-enriched precipitates and a shift in the ductile-to-brittle transformation temperature of $\Delta T_{41J} = 96$ °C after irradiation to a fluence of 5×10^{23} n m^{-2} ($E > 1$ MeV). Annealing this material for 168 h at 460 °C coarsened these Cu-enriched precipitates and recovered the embrittlement. Materials that were neutron irradiated through two cycles of 0.85×10^{23} n m^{-2} ($E > 1$ MeV) and an intermediate annealing cycle of 168 h at 460 °C also exhibited a high number density of Cu-enriched precipitates and a ΔT_{41J} shift of 56 °C. The stress relief treatment, matrix copper content of the alloy and the parameters (fluence, flux, temperature and time) of the first irradiation and the annealing treatment control copper content of the matrix and together with the parameters (fluence, flux, temperature and time) of the reirradiation control the level of this reembrittlement. Annealing this reirradiated material for 168 h at 460 °C coarsened these precipitates and recovered the embrittlement.

Acknowledgement

The authors would like to thank Drs R. Dietmar Kalkhof and Markus Niffenegger of the Paul Scherrer Institute, Switzerland and Philip Tipping of the Swiss Federal Nuclear Safety Inspectorate for their significant contributions to the research presented in this paper. Research at the Oak Ridge National Laboratory SHaRE User Facility was sponsored by the Division of Materials Sciences and Engineering (atom probe), US Department of Energy, under contract DE-AC05-00OR22725 with UT-Battelle, LLC and by the Office of Nuclear Regulatory Research, US Nuclear Regulatory Commission under interagency agreement DOE 1886-N695-3W with the US Department of Energy.

References

[1] M.K. Miller, P. Pareige, M.G. Burke, Mater. Charact. 44 (2000) 235.

[2] M.K. Miller, M.G. Hetherington, M.G. Burke, Metall. Trans. 20A (1989) 2651.
[3] J.R. Hawthorne, in: Conf. Steels for Reactor Pressure Circuits, Special Report 69, Iron and Steel Institute for the British Nuclear Energy, 1961, p. 343.
[4] J.R. Hawthorne, H.E. Watson, F.L. Loss, in: J.A. Sprague, D. Kramer (Eds.), Effects of Radiation on Structural Materials, ASTM STP 683, American Society for Testing and Materials, Philadelphia, PA, 1978, p. 278.
[5] J.R. Hawthorne, H.E. Watson, F.L. Loss, in: D. Kramer, H.R. Prager, J.S. Perrin (Eds.), Proc. 10th Conf. on Effects of Radiation in Materials, ASTM STP 725, American Society for Testing and Materials, Philadelphia, PA, 1981, p. 63.
[6] R.G. Lott, T.R. Mager, R.P. Shogan, S.E. Yanichko, in: L.E. Steele (Ed.), Radiation Embrittlement of Nuclear Reactor Pressure Vessel Steels, An International Review, vol. 2, ASTM STP 909, American Society for Testing and Materials, Philadelphia, PA, 1986, p. 242.
[7] J.R. Hawthorne, in: F.A. Garner, C.H. Hanager, N. Igata (Eds.), Symp. Influence of Radiation on Materials Properties Part II, ASTM STP 956, American Society for Testing and Materials, Philadelphia, PA, 1987, p. 461.
[8] J.R. Hawthorne, A.L. Hiser, in: D. Cubicciotti, E.P. Simonen, R.E. Gold (Eds.), Proc. 5th Int. Symp. On Environmental Degradation of Materials in Nuclear Power Systems-Water Reactors, Monterey 1991, American Nuclear Society, La Grange Park, IL, 1992, p. 671.
[9] G.R. Odette, G.E. Lucas, Rad. Effects Defects Solids 144 (1–4) (1998) 189.
[10] E. Mader, G.E. Lucas, G.R. Odette, in: Effects of Radiation on Materials: 15th International Symposium, ASTM STP 1125, 1992, p. 151.
[11] M.A. Sokolov, S. Spooner, G.R. Odette, B.D. Wirth, G.E. Lucas, in: Effects of Radiation on Materials: 18th International Symposium, ASTM STP 1325, 1999, p. 333.
[12] E.E. Eason, J.E. Wright, G.R. Odette, Nucl. Eng. Des. 179 (1998) 257.
[13] M.K. Miller, K.F. Russell, J. Nucl. Mater. 250 (1997) 223.
[14] P. Pareige, R.E. Stoller, K.F. Russell, M.K. Miller, J. Nucl. Mater. 249 (1997) 165.
[15] M.K. Miller, K.F. Russell, P. Pareige, in: G.E. Lucas, L. Snead, M.A. KirkJr., R.G. Elliman (Eds.), Proc. MRS 2000 Fall Meeting, Symposium R: Microstructural Processes in Irradiated Materials, Boston, MA, 27–30 November 2000, vol. 650, Materials Research Society, Pittsburgh, PA, 2001, p. R3.15.1.
[16] P. Pareige, B. Radiguet, A. Suvorov, M. Kozodaev, E. Krasikov, O. Zabusov, J.P. Massoud, Surf. Interf. Anal. 36 (2004) 581.
[17] M.K. Miller, Atom Probe Tomography: Analysis at the Atomic Level, Kluwer Academic/Plenum, New York, NY, 2000.
[18] M.K. Miller, A. Cerezo, M.G. Hetherington, G.D.W. Smith, Atom Probe Field Ion Microscopy, Oxford University, Oxford, UK, 1996.
[19] M.K. Miller, K.F. Russell, Surf. Interf. Anal., in press.
[20] M.K. Miller, P. Pareige, in: G.E. Lucas, L. Snead, M.A. KirkJr., R.G. Elliman (Eds.), Proc. MRS 2000 Fall Meeting, Symposium R: Microstructural Processes in Irradiated Materials, Boston, MA, 27–30 November 2000, vol. 650, Materials Research Society, Pittsburgh, PA, 2001, p. R6.1.1.
[21] J.M. Hyde, C.A. English, in: G.E. Lucas, L. Snead, M.A. KirkJr., R.G. Elliman (Eds.), Proc. MRS 2000 Fall Meeting, Symposium R: Microstructural Processes in Irradiated Materials, Boston, MA, 27–30 November 2000, vol. 650, Materials Research Society, Pittsburgh, PA, 2001, p. R6.6.1.
[22] M.K. Miller, S.S. Babu, M.A. Sokolov, R.K. Nanstad, S.K. Iskander, Mater. Sci. Eng. A 327 (2002) 76.
[23] M.K. Miller, M.A. Sokolov, R.K. Nanstad, S.K. Iskander, in: Proc. 10th Int. Conf. on Environmental Degradation of Materials in Nuclear Power Systems – Water Reactors, Lake Tahoe, NV, 5–9 August 2001, NACE, 2002.
[24] M.G. Burke, R.J. Stofanak, J.M. Hyde, C.A. English, W.L. Server, in: Proc. 10th Int. Conf. on Environmental Degradation of Materials in Nuclear Power Systems – Water Reactors, Lake Tahoe, NV, 5–9 August 2001, NACE, 2002.
[25] R.G. Carter, N. Soneda, K. Dohi, J.M. Hyde, C.A. English, W. Server, J. Nucl. Mater. 398 (2001) 211.
[26] P. Auger, P. Pareige, S. Welzel, J.C. Van Duysen, J. Nucl. Mater. 280 (2000) 331.
[27] J.M. Hyde, D. Ellis, C.A. English, T.J. Williams, in: S.T. Rosinski, M.L. Grossbeck, T.R. Allen, A.S. Kumar (Eds.), 20th Int. Conf. Effects of Radiation on Materials, ASTM STP 1405, American Society for Testing and Materials, West Conshohocken, PA, 2001, p. 262.
[28] M.A. Sokolov, R.K. Nanstad, in: R.K. Nanstad, M.L. Hamilton, F.A. Garner, A.S. Kumar (Eds.), Effects of Radiation on Materials: 18th International Symposium, ASTM STP 1325, American Society for Testing and Materials, West Conshohocken, PA, 1999, p. 167.
[29] R.K. Nanstad, M. Niffenegger, R.D. Kalkhof, M.K. Miller, M.A. Sokolov, P. Tipping, J. ASTM Int. 2 (9) (2005), paper ID JAI12888.
[30] P. Tipping, R. Cripps, in: R. Gillot (Ed.), Pressure Vessel Annealing for Plant Life Management (PLM); Tensile and Hardness Properties of Irradiated, Annealed and Reirradiated Low Alloy Steel, Trans. 12th Intl. Conf. on Structural Mechanics in Reactor Technology, SMIRT (Stuttgart), 1993, vol. DG03/3, p. 409.
[31] R.K. Nanstad, P. Tipping, R.D. Kalkhof, M.A. Sokolov, in: M.L. Grossbeck (Ed.), Effects of Radiation on Materials: 21st International Symposium, ASTM STP 1447, American Society for Testing and Materials, West Conshohocken, PA, 2004.